

Synthesis and Design of Carbon Quantum Dots/CdS/ZnS photoanode Thin Films based Solar Cells with Cu-CuS Count Electrode for a Green Environment

AKAUN Ifeanyi Patricia^{*1}, OPENE nkechi Josephine², OKUNZUWA Ikponmwosa Samuel³,
EJERE A. A.,³ OKOLI Nonso Livinus⁴ and ALU Noble Okezika⁵

Department of Art and Humanities, Delta State Polytechnic, Ogwashi-Uku, Delta State Nigeria¹

Department of Science Laboratory Technology, Delta State Polytechnic, Ogwashi-Uku, Delta State, Nigeria²

Department of Physics, Faculty of Physical Sciences, University of Benin, Benin City, Nigeria³

Department of Computer Science Education, Madonna University Nigeria, Okija Campus, Anambra State, Nigeria⁴

Sheda Science and Technology Complex (SHESTCO) Abuja, Nigeria⁵

Abstract: This study explores the synthesis and characterization of a Carbon Quantum Dots (CQDs)/CdS/ZnS photoanode thin-film solar cell with a Cu-CuS counter electrode, targeting eco-friendly and efficient photovoltaic applications. The CQDs were synthesized via a hydrothermal method, while CdS and ZnS layers were deposited using the SILAR technique. The fabricated solar cell, comprising FTO/d-TiO₂/m-TiO₂/CQD/CdS/ZnS//CuS-Cu, demonstrated a short-circuit current density (J_{sc}) of 26.30 μ A, an open-circuit voltage (V_{oc}) of 0.470 V, and a power conversion efficiency (PCE) of 1.88%. The Cu-CuS counter electrode show cased desirable electronic properties, including a low resistivity (ρ) of $2.161 \times 10^{-2} \Omega\text{-cm}$ and high conductivity (σ) of $4.628 \times 10^2 \text{ S/cm}$, Hall coefficient (R_H) of value of $5.659 \text{ cm}^3/\text{C}$ and sheet resistance (R_s) value of $3.087 \Omega/\text{sq}$. These findings suggest that incorporating green materials and innovative design can significantly contribute to sustainable energy solutions, though further optimizations are required to enhance device performance.

1.0 INTRODUCTION

The growing global focus on sustainability and environmental conservation has brought green synthesis of nanomaterials into the spotlight as a crucial approach in modern nanotechnology [1,2]. Among renewable energy sources, solar energy is particularly promising due to its abundance thereby offering approximately 120,000 terawatts of power to Earth's surface, which is 6,000 times the world's current energy consumption [3]. Solar cell as a device that is capable of converting sunlight into electricity through the photovoltaic (PV) effect have seen significant progressions in recent times [4,5]. This advancements include the development of different categories such as perovskite solar cells [6-11], organic/polymer solar cells [12-14], quantum dot solar cells [15-18], flexible solar cells [19-21], tandem solar cells [22-24] and many other architectures. These advanced PV technologies offer diverse applications like foldable chargers, wearable devices and transparent curtains which addressing the need for adaptable and innovative energy solutions. One of such advances in recent time is carbon quantum dots (CQDs).

Carbon quantum dots (CQDs) are small, carbon-based nanoparticles typically less than 10 nanometers in size [25]. These nanomaterials possess unique properties, including strong fluorescence, biocompatibility, and low toxicity, making them highly suitable for various applications such as bioimaging, sensing, drug delivery, and energy devices like solar cells [26]. Carbon quantum dots (CQDs) have become a more environmentally friendly option than standard semiconductor quantum dots (SQDs) which frequently include dangerous elements like lead (Pb) and cadmium (Cd) [27, 28]. Because of their great charge transfer capabilities, broad absorption spectra, huge two-photon absorption cross-section, and good photostability, CQDs are especially valued for their effectiveness in preventing electron-hole pair recombination in solar cells [29].

CQDs can also perform a variety of functions in photovoltaic devices, including interlayer spacing components that align energy levels across various functional layers, light absorbers, and electron donors/acceptors [30-33]. The integration of CQDs into various layers of solar cells such as electron-transporting layers (ETL), active absorbing layers, hole-transporting layers (HTL), and energy level alignment interlayers [34-36] has shown great potential in enhancing device performance while ensuring environmental safety. Compared to cadmium sulfide (CdS) and zinc sulfide (ZnS) QDs which provide strong electron transport properties and stability, CQDs are more appealing for environmentally friendly and scalable production.

The bottom-up hydrothermal synthesis of carbon quantum dots (CQDs) from citric acid and ammonia (or nitrogen sources) has garnered significant attention due to its potential applications in optoelectronics and biomedicine [37-39]. Various studies had highlighted the effectiveness of citric acid as a carbon precursor and the role of nitrogen doping in enhancing the properties of CQDs [40-44]. Other synthetic approaches that have been employed to synthesize CQDs include green synthesis [45-38], pyrolysis technique [49-51], microwave assisted [52, 53], electrochemical carbonization [54-55], laser ablation [56-57] and chemical oxidation [58-59].

In the other hand, CdS and ZnS thin films are binary semiconductors with unique properties suitable for their application in solar cells and other optoelectronic application. Cadmium sulfide (CdS) thin film has a direct bandgap of about 2.4 eV, making it highly suitable for optoelectronic applications [60-61]. It exhibits excellent light absorption properties in the visible spectrum and typically used as a window layer in thin-film solar cells due to its ability to transmit light efficiently while forming a heterojunction with other materials like cadmium telluride or copper indium gallium selenide [62-66]. These heterojunctions facilitate efficient charge separation and collection thereby improving the overall performance of solar cells. Zinc sulfide (ZnS) is a wide-bandgap material with a bandgap of approximately 3.65 eV, making it transparent to visible light and suitable for applications requiring high optical transparency and luminescence [67]. In solar cells, ZnS is often used as a buffer or window layer in tandem with materials [64] or other thin film technologies. Its role is to enhance light transmission and serve as an electron transport layer, contributing to the efficiency and stability of the device [68-69]. CdS/ZnS heterojunction thin films combining the advantageous properties of both binary semiconductor. These heterojunctions are created by layering CdS and ZnS, forming a junction that exhibits excellent properties for solar cell application [70-71].

In this work, we focused on developing low cost and efficient solar cells using Carbon Quantum Dots (CQDs)/CdS/ZnS trilayer thin films with Cu-CuS counter electrodes. CQDs, being non-toxic and cost-effective, enhance light absorption and sustainability, while ZnS reduces environmental risks associated with cadmium. The Cu-CuS counter electrode offers a low-cost, scalable alternative to rare materials, improving the commercial viability of the cells. This approach combines green materials and innovative design to promote renewable energy solutions for a sustainable future.

2.0 EXPERIMENTAL DETAILS

Reagents and other materials used for the fabrication of the solar cell include Ti-nanoxide D/SP (solaronix), titanium (IV) isopropoxide (Aldrich), Zr-nanoxide Z/SP (solaronix), Elcocarb B/SP (solaronix), Methanol (Aldrich), citric acid (MERCK), ammonia (MERCK), zinc acetate (MERCK), cadmium chloride (Aldrich), sodium sulphide (Aldrich), Ammonium solution (Aldrich), Distilled water, Fluorine doped Tin Oxide transparent conducting glass TCO30-8 (Solaronix), Acetylacetone (MERCK), Titanium (IV) chloride (MERCK),

2.1 Solar cell Fabrication

Prior to fabrication of the solar cell, the FTO substrates used underwent cleaning through a series of steps, including washing in a detergent solution, rinsing with distilled water, a final wash with isopropanol, and drying using a spin coater (Labscience model 800) at 3000 RPM. The cleaned FTO was masked to create a cell of 4 x 8 mm.

2.1.1 Deposition of dense TiO₂ thin film layer

TiO₂ thin film was deposited using electrostatic spray pyrolysis. The substrate temperature was set at 400°C, with a precursor flow rate of 0.1ml/min, atomizing voltage of 8kv, and a substrate to nozzle distance of 20mm. A total of 0.3ml of the precursor was sprayed. The precursor composition was made up of 0.15M titanium (IV) isopropoxide, 0.30 M acetylacetone and methanol was used as solvent.

2.1.2 Deposition of Mesoporous TiO₂ thin film layer

Ti-nanoxide was applied by screen printing, followed by annealing at 500°C for 30 minutes to prepare mesoporous TiO₂ (m-TiO₂). The formed m-TiO₂ film was treated with a 70 mM solution of TiCl₄ at 70°C for 30min, rinsed with water, and annealed at 100 °C for 30 minutes.

2.1.3 Synthesis of Carbon Quantum Dots

To synthesize carbon quantum dots, hydrothermal method of synthesis was adopted. Citric acid mixed with ammonia and distilled water was used as reagents. Firstly, 3.0 grams of citric acid was mixed with 12 mL of ammonia solution. The mixture was stirred for 20 minutes to have a homogenous mixture. 100 mL of distilled water was added gradually to the mixture under continuous stirring for another 10 minutes. The final solution was heated at 200 °C for 3 hours in a hydrothermal chamber. Formation of carbon quantum dot is confirmed by the brownish black colour observed. The CQD is dried and grinded. CQD is extracted with methanol as a solvent and purified by centrifugation. The CQD solution is stored in a test tube.

2.1.4 SILAR synthesis of CdS and ZnS thin films layers

Cadmium sulphide (CdS) and zinc sulphide (ZnS) thin films were synthesized using successive ionic layer adsorption reaction (SILAR). These were achieved using aqueous solutions of 0.10 M of cadmium chloride and 0.10 M of zinc acetate as precursors of Cd and Zn ions respectively. Sodium Sulfide was used as a source of S²⁻ ions. The pH of metal ions were adjusted to 8.0 using sufficient quantity of concentrated NH₄OH solution. Four steps SILAR cycle approach similar to the steps used by [72-74] were used to synthesize the binary metal sulphides of CdS and ZnS thin films.

2.1.5 Synthesis of CuS-Cu counter electrode thin film

Cu-CuS layer was assembled on Ni-Co-Cu mesh substrate by immersion in 0.5M sodium sulphide solution for 30 minutes. The reaction forms a surface layer of copper sulphide.

2.2 Assembly of carbon quantum dot sensitized solar cell (CQDSSC) with CuS-Cu

The CQDSSC is assembled by sandwiching these layers as shown in figure 1. The counter electrode is then attached with a glue and the electrolyte filled through a hole drilled on the counter electrode. The CQDSSC architecture is made up of FTO/d-TiO₂/m-TiO₂/CQD/CdS/ZnS/CuS-Cu as shown in figure 1(a). The prototype design is shown in figure 1(b). The synthesized solar cell is made of 6 Silar cycles of CdS and 2 of ZnS. The developed CQDSSC was characterized to determine the cell parameters such as power conversion efficiency (η), open circuit voltage (V_{oc}), short circuit current (J_{sc}), fill factors and others.

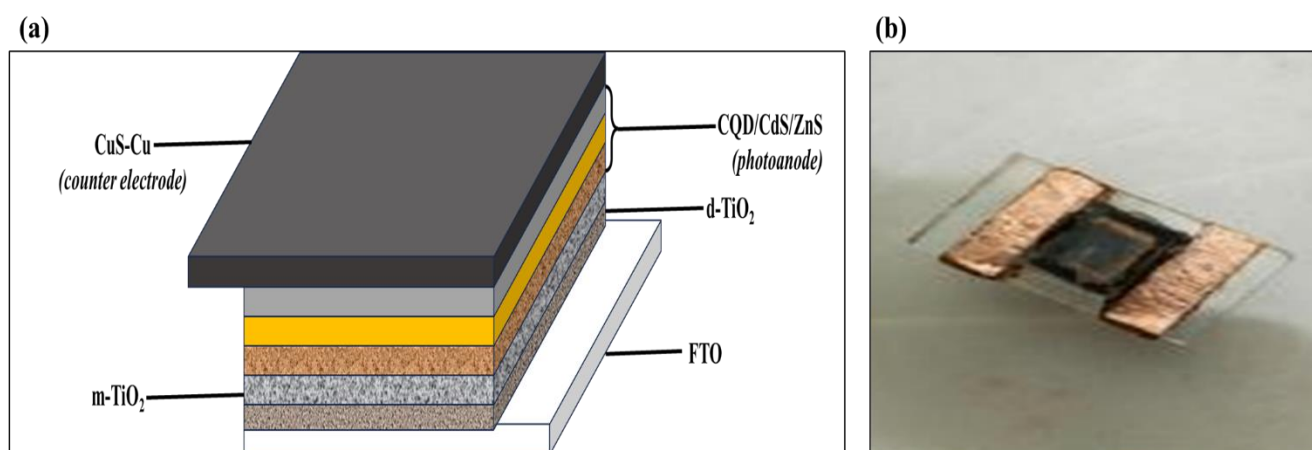


Figure 1: Assembled QDSSC (a) designed structure and (b) prototype

3.0 RESULTS AND DISCUSSIONS

3.1 Solar cell parameters

To determine the properties of the fabricated FTO/d-TiO₂/m-TiO₂/CQD/CdS/ZnS/CuS-Cu (6 cycle of CdS and 2 cycle of ZnS) CQDSSC, the current and voltage measurement of the cell was down. I-V curve was obtained under irradiance intensities of

1000 W/m² at 25 °C. For an ideal solar cell, the light-induced current generated (I_{ph}) is closely linked to the incident photon flux on the photodiode by the equation (1) as given by [75]

$$I = I_{ph} - I_d$$

$$I = I_{ph} - I_0 \left[e^{\frac{qV}{kT}} - 1 \right] \tag{1}$$

Where I_d is diode current, K_B is boltzman constant, T is absolute temperature, q is the electron charge, V is voltage at terminals and I_0 is saturation current. The short circuit current (J_{sc}) is equal to the light-generated current (I_{ph}). In this case, the open-circuit voltage (V_{oc}) can be calculated using equation (2) as given by [75]

$$V_{oc} = \frac{k_B T}{q} \ln \left(1 - \frac{I_{ph}}{I_0} \right) \tag{2}$$

The short-circuit current (I_{sc}) is the current when the voltage across the cell is at its minimum (zero) and the current is at its maximum. The open-circuit voltage (V_{oc}) is the voltage when the cell is not connected to any load. The fill factor (FF) is given in equation (3) by [76-77]

$$FF = \frac{I_{mp} \times V_{mp}}{J_{sc} \times V_{oc}} \tag{3}$$

Where I_{mp} is the maximum power current and V_{mp} is the maximum power voltage. The power conversion efficiency of the solar cell is given in equation (4) by [76-77]

$$\eta = \frac{P_{max}}{P_{in}} = \frac{V_{oc} \times J_{sc} \times FF}{\text{incident solar power } (P_{in})}$$

The I-V measurement of CuS-S counter electrode based solar cell was carried out using solar simulation equipment at SHESTCO, Abuja Nigeria. The solar simulation parameters used were flux intensity of 1000 W/m² and AM1.5 solar spectrum. The IV results obtained were plotted and solar parameter determine d from the plot. The area of the solar cell was found to be 32 mm². Figure 2 shows the I-V curve of the solar cell while table 1 gives the corresponding solar cell parameters obtained from Figure 2.

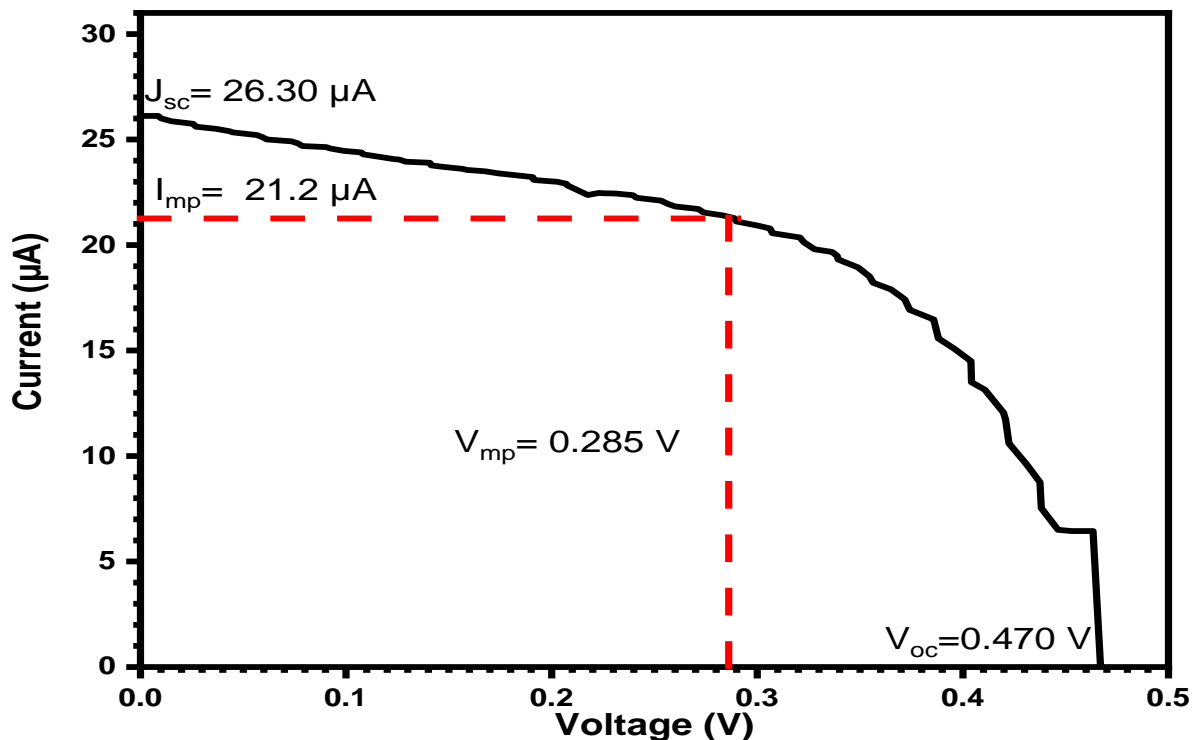


Figure 2: I-V curve of FTO/d-TiO₂/m-TiO₂/CQD/CdS/ZnS/CuS-Cu (6 cycle of CdS and 2 cycle of ZnS) CQDSSC

Table 1: Solar cell parameters of FTO/d-TiO₂/m-TiO₂/CQD/CdS/ZnS/CuS-Cu (6 cycle of CdS and 2 cycle of ZnS) CQDSSC

Cell name	J_{sc} (μA)	V_{oc} (V)	I_{mp} (μA)	V_{mp} (V)	P_{max} (μW)	P_{in} (W)	FF	η (%)
CuS-Cu	26.30	0.470	21.20	0.285	6.04	0.032	0.489	1.88

The performance of the FTO/d-TiO₂/m-TiO₂/CQD/CdS/ZnS/CuS-Cu quantum dot sensitized solar cell (QDSSC) was evaluated, yielding a short-circuit current density (J_{sc}) of 26.30 μA and an open-circuit voltage (V_{oc}) of 0.470 V, with a maximum power output (P_{max}) of 6.04 μW at a current (I_{mp}) of 21.20 μA and voltage (V_{mp}) of 0.285 V. The solar cell demonstrated a fill factor (FF) of 0.489 and a power conversion efficiency (PCE) of 1.88%, calculated against an input power (P_{in}) of 0.032 W. These results highlight the cell's moderate efficiency, typical of quantum dot-based solar cells, and point to areas for improvement, such as reducing resistive losses to increase the FF and efficiency. The stable I-V curve indicates minimal shunt resistance losses, though the gap between J_{sc} and I_{mp} suggests some series resistance impacts performance. Similar researches [78-80] have shown that PCE of CQDSSC is generally low. Liu et al [78] reported a PCE of 1.61% for QDSSC on a vertical TiO₂ nanotubes. Mistry et al [79] reported a PCE of 1.20% for nitrogen doped QDSSC. Alavi et al [80] reported an improved PEC values that ranged between 2.52 and 4.62% for QDSSC with similar TiO₂/CdS/ZnS photoanode combinations but different counter electrode.

3.2 Hall effect measurement and I-V curve of counter electrode material

Figure 3 (a) and table 2 show the I-V and hall measurement parameters of CuS-Cu electrode. The Hall effect parameters of CuS-Cu thin films provide critical insights into their electronic and transport properties, particularly their potential as counter electrodes in quantum dot solar cells. The carrier concentration (n_b) of $1.103 \times 10^{18} \text{ cm}^{-3}$ suggests sufficient charge carriers for conduction, which is essential for maintaining efficient electron transfer during solar cell operation. The moderate mobility of $2.619 \times 10^2 \text{ cm}^2/\text{Vs}$ indicates some level of scattering, which can be minimized to optimize performance.

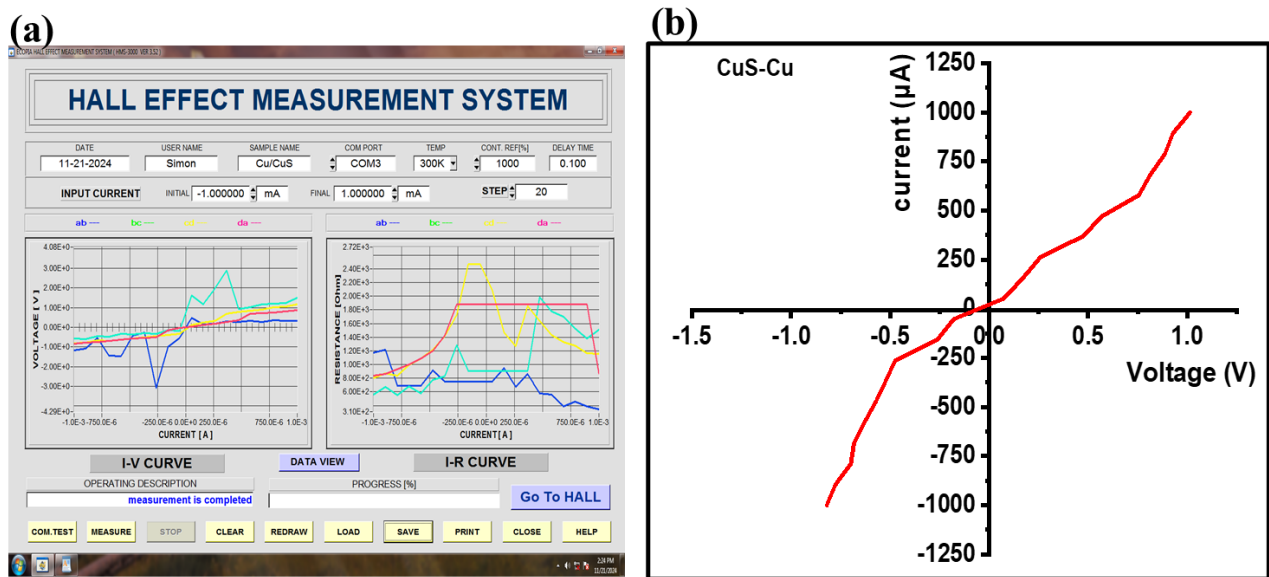


Figure 3(a-b): Hall effect measurement of and I-V curve of CuS-Cu counter electrode

The low resistivity (ρ) = $2.161 \times 10^{-2} \Omega\cdot\text{cm}$ and high conductivity (σ) of $4.628 \times 10^2 \text{ S/cm}$ demonstrate efficient charge transport, a desirable characteristic for counter electrodes which require low electrical resistance for high current flow. The Hall coefficient (R_H) of value of $5.659 \text{ cm}^3/\text{C}$ provides clues about the majority carrier type, likely electrons or holes, critical for matching the band alignment in quantum dot solar cells.

Additionally, sheet resistance (R_s) value of $3.087 \Omega/\text{sq}$ confirm the material's suitability for thin-film applications. These properties imply that Cu-CuS thin films can efficiently catalyze the redox reactions at the counter electrode while maintaining electrical stability. This makes them a promising alternative to conventional materials like platinum, offering a cost-effective and scalable solution for next-generation solar cells. Optimizing these parameters could further improve their catalytic activity and energy conversion efficiency, enhancing the performance of quantum dot solar cells.

Table 2: Hall effect parameters of the deposited Cu-CuS thin films

$n_b \times 10^{18} \text{ (cm}^{-3}\text{)}$	$\mu \times 10^2 \text{ (cm}^2/\text{Vs}\text{)}$	$\rho \times 10^{-2} \text{ (\Omega cm)}$	$R_H \text{ (cm}^3/\text{C}\text{)}$	$n_s \times 10^{15} \text{ (cm}^{-3}\text{)}$	$\sigma \times 10^1 \text{ (S/cm)}$	$R_s \text{ (\Omega/sq)}$
1.103	2.619	2.161	5.659	7.721	4.628	3.087

4.0 CONCLUSION

This study successfully fabricated and characterized a Carbon Quantum Dots (CQDs)/CdS/ZnS trilayer thin-film solar cell incorporating a Cu-CuS counter electrode. The solar cell demonstrated a power conversion efficiency (PCE) of 1.88%, a short-circuit current density (J_{sc}) of 26.30 μA , and an open-circuit voltage (V_{oc}) of 0.470 V under standard test conditions. The Cu-CuS counter electrode exhibited excellent electrical properties, including a low resistivity (ρ) of $2.161 \times 10^{-2} \Omega\text{-cm}$ and high conductivity (σ) of $4.628 \times 10^2 \text{ S/cm}$, Hall coefficient (R_H) of value of $5.659 \text{ cm}^3/\text{C}$ and sheet resistance (R_s) value of 3.087 Ω/sq emphasizing its potential for scalable photovoltaic applications. When compared with other studies, the obtained PCE is in line with typical quantum dot-sensitized solar cells (QDSSCs). For instance, Liu et al. reported a PCE of 1.61% for QDSSCs using vertically ranged TiO_2 nanotubes, while Mistry et al. achieved 1.20% efficiency with nitrogen-doped QDSSCs. Alavi et al. demonstrated higher efficiencies ranging from 2.52% to 4.627% using manganese-doped ZnS passivation layers and co-sensitized zinc-porphyrin photoanodes. These results highlight that while the current study aligns with existing literature, further optimization, particularly in reducing resistive losses and enhancing light absorption in the CQD layer, is essential to bridge the efficiency gap with advanced designs. This work underscores the potential of combining green synthesis approaches with innovative material design to develop eco-friendly and cost-effective solar cells.

REFERENCES

- [1] Sundararajan, N., Habeebsheriff, H. S., Dhanabalan, K., Cong, V. H., Wong, L. S., Rajamani, R., & Dhar, B. K. (2023). Mitigating Global Challenges: Harnessing Green Synthesized Nanomaterials for Sustainable Crop Production Systems. *Global challenges (Hoboken, NJ)*, 8(1), 2300187. <https://doi.org/10.1002/gch2.202300187>
- [2] Osman, A. I., Zhang, Y., Farghali, M., Rashwan, A. K., Eltaweil, A. S., Abd El-Monaem, E. M., Mohamed, I. M. A., Badr, M. M., Ihara, I., Rooney, D. W., & Yap, P.-S. (2024). Synthesis of green nanoparticles for energy, biomedical, environmental, agricultural, and food applications: A review. *Environmental Chemistry Letters*, 22(2), 841-887. <https://doi.org/10.1007/s10311-023-01682-3>
- [3] Grätzel M. (2009). Recent advances in sensitized mesoscopic solar cells. *Accounts of chemical research*, 42(11), 1788–1798. <https://doi.org/10.1021/ar900141y>
- [4] Panagoda, L. P. S. S., Sandeepa, R. A. H. T., Perera, W. A. V. T., Sandunika, D. M. I., Siriwardhana, S. M. G. T., Alwis, M. K. S. D., & Dilka, S. H. S. (2023). Advancements in photovoltaic (PV) technology for solar energy generation. *Journal of Research in Technology and Engineering*, 4(3), 30-72.
- [5] Dixit, A., Saxena, A., Sharma, R., Behera, D., & Mukherjee, S. (2023). Solar photovoltaic principles. In B. I. Ismail (Ed.), *Solar PV Panels* (Ch. 1). IntechOpen. <https://doi.org/10.5772/intechopen.109730>
- [6] Kim, D. I., Lee, J. W., Jeong, R. H., & Boo, J. H. (2022). A high-efficiency and stable perovskite solar cell fabricated in ambient air using a polyaniline passivation layer. *Scientific Reports*, 12(1), 697. <https://doi.org/10.1038/s41598-021-04547-3>
- [7] Cao, F., Bian, L., & Li, L. (2024). Perovskite solar cells with high-efficiency exceeding 25%: A review. *Energy Materials and Devices*, 2(1), 9370018. <https://doi.org/10.26599/EMD.2024.9370018>
- [8] Weerasinghe, H. C., Macadam, N., Kim, J.-E., Sutherland, L. J., Angmo, D., Ng, L. W. T., Scully, A. D., Glenn, F., Chantler, R., Chang, N. L., Dehghanimadvar, M., Shi, L., Ho-Baillie, A. W. Y., Egan, R., Chesman, A. S. R., Gao, M., Jasieniak, J. J., Hasan, T., & Vak, D. (2024). The first demonstration of entirely roll-to-roll fabricated perovskite solar cell modules under ambient room conditions. *Nature Communications*, 15(1), 1656. <https://doi.org/10.1038/s41467-024-46016-1>
- [9] Zhou, J., Tan, L., Liu, Y., Li, H., Liu, X., Li, M., Wang, S., Zhang, Y., Jiang, C., Hua, R., Tress, W., Meloni, S., & Yi, C. (2024). Highly efficient and stable perovskite solar cells via a multifunctional hole transporting material. *Joule*, 8(6), 1691-1706. <https://doi.org/10.1016/j.joule.2024.02.019>
- [10] Zheng, X., Kong, W., Wen, J., Hong, J., Luo, H., Xia, R., Huang, Z., Luo, X., Liu, Z., Li, H., Sun, H., Wang, Y., Liu, C., Wu, P., Gao, H., Li, M., Bui, A. D., Mo, Y., Zhang, X., ... Tan, H. (2024). Solvent engineering for scalable fabrication of perovskite/silicon tandem solar cells in air. *Nature Communications*, 15(1), 4907. <https://doi.org/10.1038/s41467-024-49351-5>
- [11] Rossi, F., Rotondi, L., Stefanelli, M., Sinicropi, A., Vesce, L., & Parisi, M. L. (2024). Comparative life cycle assessment of different fabrication processes for perovskite solar mini-modules. *EPJ Photovoltaics*, 15, Article 20. <https://doi.org/10.1051/epjpv/2024014>
- [12] Zeng, R., Zhu, L., Zhang, M., Zhong, W., Zhou, G., Zhuang, J., Hao, T., Zhou, Z., Zhou, L., Hartmann, N., Xue, X., Jing, H., Han, F., Bai, Y., Wu, H., Tang, Z., Zou, Y., Zhu, H., Chen, C.-C., Zhang, Y., & Liu, F. (2023). All-polymer organic solar cells with nano-to-micron hierarchical morphology and large light receiving angle. *Nature Communications*, 14(1), 4148. <https://doi.org/10.1038/s41467-023-39832-4>

- [13] Marlow, P., Manger, F., Fischer, K., Sprau, C., & Colsmann, A. (2022). Eco-friendly fabrication of organic solar cells: Electrostatic stabilization of surfactant-free organic nanoparticle dispersions by illumination. *Nanoscale*, 14(14), 5569-5578. <https://doi.org/10.1039/D2NR00095D>
- [14] Supriyanto, A., Mustaqim, A., Agustini, M., Ramelan, A. H., Suyitno, Rosa, E. S., Yofentina, & Nurosyid, F. (2016). Fabrication of organic solar cells with design blend P3HT: PCBM variation of mass ratio. IOP Conference Series: Materials Science and Engineering, 107, 012050. <https://doi.org/10.1088/1757-899X/107/1/012050>
- [15] Jiang, Y., Dai, Y., Wang, Q., & Dai, J. (2022). Fabrication of quantum dot-sensitized solar cells based on a transparent TiO₂ film with reasonable load resistance design. *ACS Applied Energy Materials*, 5(10), 12297-12304. <https://doi.org/10.1021/acsaem.2c01847>
- [16] Kumar, P. N., Das, A., Kolay, A., & Deepa, M. (2022). Simple strategies deployed for developing efficient and stable solution processed quantum dot solar cells. *Materials Advances*, 3(5), 2249-2267. <https://doi.org/10.1039/D1MA00851J>
- [17] Chernomordik, B. D., Marshall, A. R., Pach, G. F., Luther, J. M., & Beard, M. C. (2017). Quantum dot solar cell fabrication protocols. *Chemistry of Materials*, 29(1), 189-198. <https://doi.org/10.1021/acs.chemmater.6b02939>
- [18] Sotodeian, M., & Marandi, M. (2021). Fabrication of quantum dot-sensitized solar cells with multilayer TiO₂/PbS(X)/CdS/CdSe/ZnS/SiO₂ photoanode and optimization of the PbS nanocrystalline layer. *Journal of Materials Science: Materials in Electronics*, 32(8), 10123-10139. <https://doi.org/10.1007/s10854-021-05670-7>
- [19] Teixeira, C., Fuentes-Pineda, R., Andrade, L., Mendes, A., & Forgács, D. (2023). Fabrication of low-cost and flexible perovskite solar cells by slot-die coating for indoor applications. *Materials Advances*, 4(17), 3863-3873. <https://doi.org/10.1039/D3MA00285C>
- [20] Avilés-Betanzos, R., Oskam, G., & Pourjafari, D. (2023). Low-temperature fabrication of flexible dye-sensitized solar cells: Influence of electrolyte solution on performance under solar and indoor illumination. *Energies*, 16(15), 5617. <https://doi.org/10.3390/en16155617>
- [21] Liu, W., Liu, Y., Yang, Z., Xu, C., Li, X., Huang, S., Shi, J., Du, J., Han, A., Yang, Y., Xu, G., Yu, J., Ling, J., Peng, J., Yu, L., Ding, B., Gao, Y., Jiang, K., Li, Z., Yang, Y., Li, Z., Lan, S., Fu, H., Fan, B., Fu, Y., He, W., Li, F., Song, X., Zhou, Y., Shi, Q., Wang, G., Guo, L., Kang, J., Yang, X., Li, D., Wang, Z., Li, J., Thoroddsen, S., Cai, R., Wei, F., Xing, G., Xie, Y., Liu, X., Zhang, L., Meng, F., Di, Z., & Liu, Z. (2023). Flexible solar cells based on foldable silicon wafers with blunted edges. *Nature*, 617(7962), 717-723. <https://doi.org/10.1038/s41586-023-05921-z>
- [22] Zheng, X., Kong, W., Wen, J., Hong, J., Luo, H., Xia, R., Huang, Z., Luo, X., Liu, Z., Li, H., Sun, H., Wang, Y., Liu, C., Wu, P., Gao, H., Li, M., Bui, A. D., Mo, Y., Zhang, X., ... Tan, H. (2024). Solvent engineering for scalable fabrication of perovskite/silicon tandem solar cells in air. *Nature Communications*, 15(1), 4907. <https://doi.org/10.1038/s41467-024-49351-5>
- [23] Mariotti, S., Köhnen, E., Scheler, F., Sveinbjörnsson, K., Zimmermann, L., Piot, M., Yang, F., Li, B., Warby, J., Musienko, A., Menzel, D., Lang, F., Keßler, S., Levine, I., Mantione, D., Al-Ashouri, A., Härtel, M. S., Xu, K., Cruz, A., ... Albrecht, S. (2023). Interface engineering for high-performance, triple-halide perovskite-silicon tandem solar cells. *Science*, 381(6653), 63-69. <https://doi.org/10.1126/science.adf5872>
- [24] Zheng, J., Xue, C., Wang, G., Mahmud, M. A., Sun, Z., Liao, C., Yi, J., Qu, J., Yang, L., Wang, L., Bremner, S., Cairney, J. M., Zhang, J., & Ho-Baillie, A. W. Y. (2024). Efficient flexible monolithic perovskite-CIGS tandem solar cell on conductive steel substrate. *ACS Energy Letters*, 9(4), 1545-1547. <https://doi.org/10.1021/acsenerylett.4c00432>
- [25] Mansuriya, B. D., & Altintas, Z. (2021). Carbon Dots: Classification, Properties, Synthesis, Characterization, and Applications in Health Care-An Updated Review (2018-2021). *Nanomaterials (Basel, Switzerland)*, 11(10), 2525. <https://doi.org/10.3390/nano11102525>
- [26] Zahra, F., Qureshi, Z., Ali, M.N. (2024). Carbon Quantum Dots, Its Synthesis and Evaluation of Its Cytotoxicity. In: Garg, S., Chandra, A., Sagadevan, S. (eds) Emerging Sustainable Nanomaterials for Biomedical Applications. Springer, Cham. https://doi.org/10.1007/978-3-031-63961-6_14
- [27] Elugoke, S. E., Uwaya, G. E., Quadri, T. W., & Ebenso, E. E. (2024). Carbon quantum dots: Basics, properties, and fundamentals. In Carbon dots: Recent developments and future perspectives (pp. 3-42). American Chemical Society. <https://doi.org/10.1021/bk-2024-1465.ch001>
- [28] Dhariwal, J., Rao, G. K., & Vaya, D. (2024). Recent advancements towards the green synthesis of carbon quantum dots as an innovative and eco-friendly solution for metal ion sensing and monitoring. *RSC Sustain.*, 2(1), 11-36. <https://doi.org/10.1039/D3SU00375B>
- [29] Saputra, A. M. A., Piliang, A. F. R., Dellyansyah, Marpongahtun, Andriyani, Goei, R., H.T.S., R. R., & Gea, S. (2024). Synthesis, properties, and utilization of carbon quantum dots as photocatalysts on degradation of organic dyes: A mini review. *Catalysis Communications*, 187, 106914. <https://doi.org/10.1016/j.catcom.2024.106914>
- [30] Geng, C., Shang, Y., Qiu, J., Wang, Q., Chen, X., Li, S., Ma, W., Fan, H. J., Omer, A. A. A., & Chen, R. (2020). Carbon quantum dots interfacial modified graphene/silicon Schottky barrier solar cell. *Journal of Alloys and Compounds*, 835, 155268. <https://doi.org/10.1016/j.jallcom.2020.155268>

- [31] Kumar, P., Dua, S., Pani, B., & Bhatt, G. (2023). Application of Fluorescent CQDs for Enhancing the Performance of Solar Cells and WLEDs. *IntechOpen*. <https://doi.org/10.5772/intechopen.107474>
- [32] Wen, Y., Zhu, G., & Shao, Y. (2020). Improving the power conversion efficiency of perovskite solar cells by adding carbon quantum dots. *Journal of Materials Science*, 55(6), 2937–2946. <https://doi.org/10.1007/s10853-019-04145-9>
- [33] Xu, T., Wan, Z., Tang, H., Zhao, C., Lv, S., Chen, Y., Chen, L., Qiao, Q., & Huang, W. (2021). Carbon quantum dot additive engineering for efficient and stable carbon-based perovskite solar cells. *Journal of Alloys and Compounds*, 859, 157784. <https://doi.org/10.1016/j.jallcom.2020.157784>
- [34] Litvin, A. P., Zhang, X., Berwick, K., Fedorov, A. V., Zheng, W., & Baranov, A. V. (2020). Carbon-based interlayers in perovskite solar cells. *Renewable and Sustainable Energy Reviews*, 124, 109774. <https://doi.org/10.1016/j.rser.2020.109774>
- [35] Li, H., Shi, W., Huang, W., Yao, E.-P., Han, J., Chen, Z., Liu, S., Shen, Y., Wang, M., & Yang, Y. (2017). Carbon quantum dots/TiO_x electron transport layer boosts efficiency of planar heterojunction perovskite solar cells to 19%. *Nano Letters*, 17(4), 2328–2335. <https://doi.org/10.1021/acs.nanolett.6b05177>
- [36] Liu, J. (2022). Perovskite Cells Based on Carbon Quantum Dots: Structure, Optimization. *Highlights in Science, Engineering and Technology*, 27, 540–544. <https://doi.org/10.54097/hset.v27i.3812>
- [37] Qureshi, Z. A., Dabash, H., Ponnammma, D., & Abbas, M. K. G. (2024). Carbon dots as versatile nanomaterials in sensing and imaging: Efficiency and beyond. *Heliyon*, 10(11), e31634. <https://doi.org/10.1016/j.heliyon.2024.e31634>
- [38] Xu, J., Huang, B.-B., Lai, C.-M., Lu, Y.-S., & Shao, J.-W. (2024). Advancements in the synthesis of carbon dots and their application in biomedicine. *Journal of Photochemistry and Photobiology B: Biology*, 255, 112920. <https://doi.org/10.1016/j.jphotobiol.2024.112920>
- [39] Magesh, V., Sundramoorthy, A. K., & Ganapathy, D. (2022). Recent advances on synthesis and potential applications of carbon quantum dots. *Frontiers in Materials*, 9, 906838. <https://doi.org/10.3389/fmats.2022.906838>
- [40] Nguyen, K. G., Huš, M., Baragau, I.-A., Bowen, J., Heil, T., Nicolaev, A., Abramiuc, L. E., Sapelkin, A., Sajjad, M. T., & Kellici, S. (2024). Engineering nitrogen-doped carbon quantum dots: Tailoring optical and chemical properties through selection of nitrogen precursors. *Small*, 20(2310587). <https://doi.org/10.1002/sml.202310587>
- [41] Ozyurt, D., Al Kobaisi, M., Hocking, R. K., & Fox, B. (2023). Properties, synthesis, and applications of carbon dots: A review. *Carbon Trends*, 12, 100276. <https://doi.org/10.1016/j.cartre.2023.100276>
- [42] Olla, C., Cappai, A., Porcu, S., Stagi, L., Fantauzzi, M., Casula, M. F., Mocci, F., Corpino, R., Chiriu, D., Ricci, P. C., & et al. (2023). Exploring the impact of nitrogen doping on the optical properties of carbon dots synthesized from citric acid. *Nanomaterials*, 13(8), 1344. <https://doi.org/10.3390/nano13081344>
- [43] Jorns, M., Strickland, S., Mullins, M., & Pappas, D. (2022). Improved citric acid-derived carbon dots synthesis through microwave-based heating in a hydrothermal pressure vessel. *RSC Advances*, 12(50), 32401–32414. <https://doi.org/10.1039/D2RA06420K>
- [44] Šafranko, S., Jandel, K., Kovačević, M., Stanković, A., Dutour Sikirić, M., Mandić, Š., Széchenyi, A., Glavaš Obrovac, L., Leventić, M., Strelec, I., & et al. (2023). A facile synthetic approach toward obtaining N-doped carbon quantum dots from citric acid and amino acids, and their application in selective detection of Fe(III) ions. *Chemosensors*, 11(4), 205. <https://doi.org/10.3390/chemosensors11040205>
- [45] Manikandan, V., & Lee, N. Y. (2022). Green synthesis of carbon quantum dots and their environmental applications. *Environmental Research*, 212, 113283. <https://doi.org/10.1016/j.envres.2022.113283>
- [46] Fang, X.-W., Chang, H., Wu, T., Yeh, C.-H., Hsiao, F.-L., Ko, T.-S., Hsieh, C.-L., Wu, M.-Y., & Lin, Y.-W. (2024). Green synthesis of carbon quantum dots and carbon quantum dot-gold nanoparticles for applications in bacterial imaging and catalytic reduction of aromatic nitro compounds. *ACS Omega*, 9(22), 23573–23583. <https://doi.org/10.1021/acsomega.4c00833>
- [47] Mindivan, F., & Göktaş, M. (2023). The green synthesis of carbon quantum dots (CQDs) and characterization of polycaprolactone (PCL/CQDs) films. *Colloids and Surfaces A: Physicochemical and Engineering Aspects*, 677, 132446. <https://doi.org/10.1016/j.colsurfa.2023.132446>
- [48] Ashok Kumar, S., Dheeraj Kumar, M., Saikia, M., Renuga Devi, N., & Subramania, A. (2023). A review on plant derived carbon quantum dots for bio-imaging. *Materials Advances*, 4(18), 3951–3966. <https://doi.org/10.1039/D3MA00254C>
- [49] Wang, C., Yang, M., Shi, H., Yao, Z., Liu, E., Hu, X., Guo, P., Xue, W., & Fan, J. (2022). Carbon quantum dots prepared by pyrolysis: Investigation of the luminescence mechanism and application as fluorescent probes. *Dyes and Pigments*, 204, 110431. <https://doi.org/10.1016/j.dyepig.2022.110431>
- [50] Qin, X., Fu, C., Zhang, J., Shao, W., Qin, X., Gui, Y., Wang, L., Guo, H., Chen, F., Jiang, L., Wu, G., Bikker, F. J., & Luo, D. (2022). Direct preparation of solid carbon dots by pyrolysis of collagen waste and their applications in fluorescent sensing and imaging. *Frontiers in Chemistry*, 10, 1006389. <https://doi.org/10.3389/fchem.2022.1006389>

- [51] Marpongahtun, Gea, S., Muis, Y., Andriyani, & Piliang, A. F. (2018). Synthesis of carbon nanodots from cellulose nanocrystals oil palm empty fruit by pyrolysis method. *Journal of Physics: Conference Series*, 1120, 012071. <https://doi.org/10.1088/1742-6596/1120/1/012071>
- [52] Nazar, M., Hasan, M., Wirjosentono, B., Gani, B. A., & Nada, C. E. (2024). Microwave synthesis of carbon quantum dots from Arabica coffee ground for fluorescence detection of Fe³⁺, Pb²⁺, and Cr³⁺. *ACS Omega*, 9(18), 20571-20581. <https://doi.org/10.1021/acsomega.4c02254>
- [53] Tohamy, H. A. S., El-Sakhawy, M., & Kamel, S. (2023). Microwave-assisted synthesis of amphoteric fluorescence carbon quantum dots and their chromium adsorption from aqueous solution. *Scientific Reports*, 13, 11306. <https://doi.org/10.1038/s41598-023-37894-4>
- [54] Rocco, D., Moldoveanu, V. G., Feroci, M., Bortolami, M., & Vetica, F. (2023). Electrochemical synthesis of carbon quantum dots. *ChemElectroChem*, 10(3), e202201104. <https://doi.org/10.1002/celec.202201104>
- [55] Guzmán-López, J. E., Pérez-Isidoro, R., Amado-Briseño, M. A., Lopez, I., Villareal-Chiu, J. F., Sánchez-Cervantes, E. M., Vázquez-García, R. A., & Espinosa-Roa, A. (2024). Facile one-pot electrochemical synthesis and encapsulation of carbon quantum dots in GUVs. *Chemical Physics Impact*, 8, 100519. <https://doi.org/10.1016/j.chphi.2024.100519>
- [56] Kaczmarek, A., Hoffman, J., Morgiel, J., Mościcki, T., Stobiński, L., Szymański, Z., & Małolepszy, A. (2021). Luminescent Carbon Dots Synthesized by the Laser Ablation of Graphite in Polyethylenimine and Ethylenediamine. *Materials (Basel, Switzerland)*, 14(4), 729. <https://doi.org/10.3390/ma14040729>
- [57] Santiago, S. R. M., Lin, T. N., Chang, C. H., Wong, Y. A., Lin, C. A. J., Yuan, C. T., & Shen, J. L. (2017). Synthesis of N-doped graphene quantum dots by pulsed laser ablation with diethylenetriamine (DETA) and their photoluminescence. *Phys. Chem. Chem. Phys.*, 19(33), 22395-22400. <https://doi.org/10.1039/C7CP03993J>
- [58] Zhu, J., Zhu, M., He, Z., Xiong, L., Zhang, R., & Guo, L. (2023). Chemical oxidation synthesized high-yield carbon dots for acid corrosion inhibition of Q235 steel. *ChemistrySelect*, 8(7), e202204621. <https://doi.org/10.1002/slct.202204621>
- [59] Tan, C., Zuo, S., Zhao, Y., & Shen, B. (2019). Preparation of multicolored carbon quantum dots using HNO₃/HClO₄ oxidation of graphitized carbon. *Journal of Materials Research*, 34(20), 3428-3438. <https://doi.org/10.1557/jmr.2019.261>
- [60] Smairi, S., Hartiti, B., Arba, Y., Labrim, H., Fadili, S., Tahri, M., Belfhailli, A., & Thévenin, P. (2022). Elaboration and characterization of cadmium sulfide (CdS) thin films prepared by chemical bath deposition (CBD). *Materials Today: Proceedings*, 66, 112-115. <https://doi.org/10.1016/j.matpr.2022.03.690>
- [61] A. El Kissani, H. Ait Dads, S. Oucharrou, F. Welatta, H. Elaakib, L. Nkhaili, A. Narjis, A. Khalfi, K. El Assail, & A. Outzourhit. (2018). A facile route for synthesis of cadmium sulfide thin films. *Thin Solid Films*, 664, 66-69. <https://doi.org/10.1016/j.tsf.2018.08.034>
- [62] Mao, J., Xu, W., & Seo, S. (2024). Exploring the Dual Phases of Cadmium Sulfide: Synthesis, Properties, and Applications of hexagonal wurtzite and cubic zinc blende Crystal Structures. *Journal of Materials Chemistry A*, 12(35), 23218-23242. <https://doi.org/10.1039/d4ta03496a>
- [63] Zheng, X., Liu, Y., Yang, Y., Song, Y., Deng, P., Li, J., Liu, W., Shen, Y., & Tian, X. (2023). Recent Advances in Cadmium Sulfide-Based Photocatalysts for Photocatalytic Hydrogen Evolution. *Renewables*, 1(1), 39-56. <https://doi.org/10.31635/renewables.022.202200001>
- [64] Faremi, A. A., Akindadelo, A. T., Adekoya, M. A., Adebayo, A. J., Salau, A. O., Oluyamo, S. S., & Olubambi, P. A. (2022). Engineering of window layer cadmium sulphide and zinc sulphide thin films for solar cell applications. *Results in Engineering*, 16, 100622. <https://doi.org/10.1016/j.rineng.2022.100622>
- [65] Melchor-Robles, J. A., Nieto-Zepeda, K. E., Vázquez-Barragán, N. E., M. Arreguín-Campos, K. Rodríguez-Rosales, J. Cruz-Gómez, A. Guillén-Cervantes, J. Santos-Cruz, de, M., G. Contreras-Puente, & F. de Moure-Flores. (2024). Characterization of CdS/CdTe Ultrathin-Film Solar Cells with Different CdS Thin-Film Thicknesses Obtained by RF Sputtering. *Coatings*, 14(4), 452-452. <https://doi.org/10.3390/coatings14040452>
- [66] Ray, J., Patel, K., Bhatt, G., Suryavanshi, P., & Panchal, C. J. (2021). Fabrication of Copper Indium Gallium Diselenide (Cu(In,Ga)Se₂) Thin Film Solar Cell. *Electrical and Electronic Devices, Circuits, and Materials*, 169-187. <https://doi.org/10.1002/9781119755104.ch10>
- [67] Mukherjee, A., & Mitra, P. (2017). Characterization of Sn Doped ZnS Thin Films Synthesized by CBD. *Materials Research*, 20(2), 430-435. <https://doi.org/10.1590/1980-5373-mr-2016-0628>
- [68] Bennett, H. C., Tamilarasi R, Ashok, A., Joselin, F., Nandhakumar R, Antony, E., & R Jeba Beula. (2024). Structural and opto-electronic engineering with ZnS ETL via PVD technique for efficient and durable heterojunction perovskite solar cells. *Optical Materials*, 154, 115695-115695. <https://doi.org/10.1016/j.optmat.2024.115695>
- [69] Mude, N. N., Khan, Y., Thuy, T. T., Walker, B., & Kwon, J. H. (2022). Stable ZnS Electron Transport Layer for High-Performance Inverted Cadmium-Free Quantum Dot Light-Emitting Diodes. *ACS Applied Materials & Interfaces*, 14(50), 55925-55932. <https://doi.org/10.1021/acsmi.2c14711>

- [70] Li, C., Li, H., Zhu, Z., Yin, T., Wang, Z., Li, P., Zeng, C., Yang, F., Zhong, P., Cui, N., & Shou, C. (2022). Electric field enhanced with CdS/ZnS quantum dots passivation for efficient and stable perovskite solar cells. *Journal of Power Sources*, 537, 231519–231519. <https://doi.org/10.1016/j.jpowsour.2022.231519>
- [71] Hernández Castillo, R., Acosta, M., Riech, I., Santana-Rodríguez, G., Mendez-Gamboa, J., Acosta, C., & Zambrano, M. (2017). Study of ZnS/CdS structures for solar cells applications. *Optik*, 148, 95–100. <https://doi.org/10.1016/j.ijleo.2017.09.002>
- [72] C.J. Nkamuo, Okoli, N. L., F.N. Nzekwe, & N.J. Egwunyenga. (2024). Tuning the properties of manganese-doped zinc oxide nanostructured thin films deposited by SILAR approach. *Chemistry of Inorganic Materials*, 2, 100038–100038. <https://doi.org/10.1016/j.cinorg.2024.100038>
- [73] Eze, C. B., Ezenwa, I. A., Okoli, N. L., Elekalachi, C. I., & Okereke, N. A. (2023). Study of Optical and Structural Properties of SILAR-deposited Cobalt Sulphide Thin Films. *Journal of Nano and Materials Science Research*, 2(1), 123–130. url: <https://journals.nanotechunn.com/jnmrs/article/view/15>
- [74] Elekalachi, C. I., Ezenwa, I. A., Okereke, A. N., Okoli, N. L., & Nwori, A. N. (2022). Influence of Annealing Temperature on the Properties of SILAR Deposited CdSe/ZnSe Superlattice Thin Films for Optoelectronic Applications. *Nanoarchitectonics*, 26–44. <https://doi.org/10.37256/nat.4120231650>
- [75] Nair, K., Jose, J., Ravindran, A., & Scholar, P. (2016). Analysis of temperature dependent parameters on solar cell efficiency using MATLAB. *International Journal of Engineering Development and Research*, 4, 536-541.
- [76] Baniyounis, M. J., Mohammed, W. F., & Abuhashhash, R. T. (2022). Analysis of power conversion limitation factors of Cu (In_xGa_{1-x}) (Se)₂ thin-film solar cells using SCAPS. *Materials for Renewable and Sustainable Energy*, 11(3), 215–223. <https://doi.org/10.1007/s40243-022-00215-2>
- [77] Chen, L., Fang, C., & Liu, W. (2020). Influence of Absorption Layer Thickness on the Performance of CIGS Solar Cells. *IOP Conference Series Earth and Environmental Science*, 440(3), 032051–032051. <https://doi.org/10.1088/1755-1315/440/3/032051>
- [78] Liu, Z., Luan, W., Yuan, B., Jin, L., & Tu, S.-T. (2016). Quantum-dots-sensitized solar cells based on vertically ranged titanium dioxide nanotubes. *International Journal of Green Energy*, 13(8), 840–844. <https://doi.org/10.1080/15435075.2016.1161634>
- [79] Mistry, B., Machhi, H. K., Vithalani, R. S., Patel, D. S., Modi, C. K., Prajapati, M., Surati, K. R., Soni, S. S., Jha, P. K., & Kane, S. R. (2019). Harnessing the N-dopant ratio in carbon quantum dots for enhancing the power conversion efficiency of solar cells. *Sustainable Energy & Fuels*, 3(11), 3182–3190. <https://doi.org/10.1039/c9se00338j>
- [80] Alavi, M., Rahimi, R., Maleki, Z., & Hosseini-Kharat, M. (2020). Improvement of Power Conversion Efficiency of Quantum Dot-Sensitized Solar Cells by Doping of Manganese into a ZnS Passivation Layer and Cosensitization of Zinc-Porphyrin on a Modified Graphene Oxide/Nitrogen-Doped TiO₂ Photoanode. *ACS Omega*, 5(19), 11024–11034. <https://doi.org/10.1021/acsomega.0c00855>